RSC Advances

RSC Publishing

PAPER

View Article Online
View Journal | View Issue

Zigzag graphene nanoribbons with curved edges

Nam B. Le[ab] and Lilia M. Woods*[a]

Cite this: *RSC Advances*, 2013, **3**, 10014

Received 17th April 2013,
Accepted 3rd May 2013

DOI: 10.1039/c3ra41870g

www.rsc.org/advances

Zigzag-edged single and double folded graphene nanoribbons are studied using density functional theory methods. Some asymmetric folds and folds with an octagon/hexagonal extended defect line are also considered. The long-range van der Waals interactions are taken into account *via* semiempirical pairwise optimized potential. The geometrical and magnetic phases of the studied structures are obtained. It is shown that the magnetic states of the folds depend strongly on their stacking patterns. The electronic structures in terms of energy needed for the folding process, van der Waals contribution, energy band gaps, band structures, and densities of states are also calculated. We find that significant changes in the electronic structure can be achieved as a result of folding and adding line defects.

1 Introduction

Graphene is an atomically thin sheet of sp^2-bonded C atoms arranged in a honeycomb lattice. This material is stable under ambient conditions and it possesses exceptional mechanical, transport, and optical properties.[1,2] Graphene nanoribbons (GNRs) are quasi-one dimensional graphene derivatives with a finite width and distinct edge structure. GNR edges can have armchair or zigzag types determining their electronic structure characteristics. An unusual feature is the presence of antiferromagnetic ordering in GNRs with zigzag edges.[3–5] Both, graphene and GNRs, are considered to be promising materials for applications in novel technologies, especially for high-speed electronics.[6]

Structural engineering is an emerging tool for tailoring properties of materials, such as carbon-based systems. Creating organized extended defects or mechanical wrapping and folding of graphene structures are particularly promising methods. For instance, a line defect consisting of sp^2 C pentagons and octagons behaves as a metallic wire embedded in graphene.[7] Rolling, twisting, and folding in out of plane direction can also be achieved due to the graphene and GNR flexibility. In particular, folding can be achieved *via* mechanical stimulations,[8,9] etching[10] or high temperature annealing[11] techniques.

A topic of considerable interest is to study the interplay between the particular types of GNRs, the presence of extended defects and folding in order to find new ways to further change the properties of these functional materials. In an earlier publication,[12] we investigated folded armchaired GNRs as a function of their width. Our electronic structure calculations showed that the interlayer van der Waals (vdW) coupling together with the strain from the folding can lead to semiconductor–semi-metal transitions in the energy band structure. The interlayer dispersive interaction is registry dependent and it plays a significant role for the stability of the folded structures.

The motivation for this work is to propose additional ways to modify properties of nanoribbons combining the unusual electronic and magnetic characteristics stemming from the zigzag type of edging. In addition, the presence of pentagon/octagon extended line defects in folded zigzag GNRs is also studied to show how the properties are further evolved. Analysis and comparison of folded graphene nanoribbons with armchaired edges are also presented, in order to demonstrate the differences and similarities and highlight the zigzag edge and its magnetic nature.

2 Method and structures

The results reported here are obtained utilizing self-consistent density functional theory (DFT) calculations within the Vienna *Ab Initio* Simulation Package (VASP).[13] In this state of the art code, the Kohn–Sham equations are solved using the projector-augmented-wave (PAW) method of Blochl,[14] with a plane-wave basis set and periodic boundary conditions. The exchange–correlation energy is described by the Perdew–Burke–Ernzerhof[15] (PBE) functional. For all of our calculations, we have used a plane wave cutoff of 450 eV and a Brillouin zone sampling of $(1 \times 1 \times 7)$ automatic-mesh k-points. To ensure that each structure reaches its equilibrium state we set the total energy and force criteria to 10^{-5} eV and 10^{-2} eV Å^{-1}, respectively. Each supercell is constructed so that the distance between nearest structures in each direction is 20 Å. Increasing the size of the supercell or improving the

[a]*Department of Physics, University of South Florida, 4202 E. Fowler Avenue, Tampa, FL 33620, USA. E-mail: lmwoods@usf.edu*
[b]*Department of Theoretical Physics, Institute of Engineering Physics, Hanoi University of Science and Technology, 1 Dai Co Viet, Hanoi, Vietnam*

convergence criteria does not lead to significant changes in our results.

The long-ranged van der Waals (vdW) interaction plays a determining role in the formation and stability of the folded structures. The vdW coupling is taken into account *via* the DFT-D2 approach[16,17] implemented in VASP, with the parametrization given by Grimme *et al.*[18,19] In this method, a semiempirical dispersion potential is added to the conventional Kohn–Sham energy, and the vdW correlations are calculated self-consistently through a pairwise force field optimized for DFT functionals. Despite its two-body nature, the DFT-D2 implementation is an efficient way enabling first principles calculations to take into account vdW dispersive interactions.

The structures of interest here are zigzag GNRs with saturated by H end bonds. Each GNR is specified by the number N of its zigzag C lines extending along the axial direction, which also corresponds to a particular width W as shown in Fig. 1a. We study single and double folded symmetric ribbons Fig. 1b and 1d. Single folds in which the top N_t and bottom N_b flat portions have different size are also considered. These are termed as ''asymmetric'' structures (shown in Fig. 1c). Line defects comprised of rotated CC bonds and forming an ordered extension of two pentagons followed by an octagon are also created in the center of a zigzag GNRs Fig. 2a. Consequently, single and double folded defective GNRs are investigated, as shown in Fig. 2b and 2c.

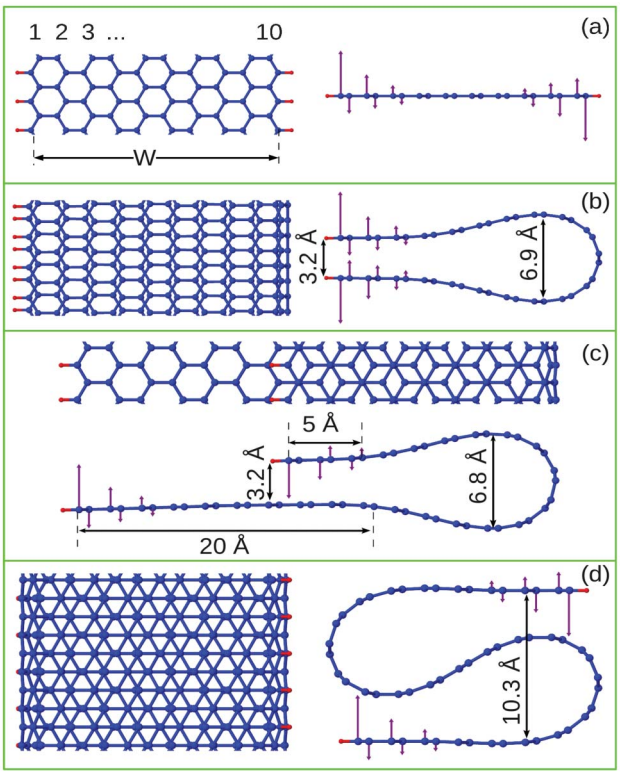

Fig. 1 Top and side views of the GNR structures: (a) unfolded ribbon with $N = 10$ zigzag C lines; (b) single folded ribbons with $N = 21$ C lines; (c) asymmetrically single folded ribbon with $N = 26$ ($N_t = 3$ C lines on top and $N_b = 10$ C lines on bottom in the flat region); (d) double folded ribbon with $N = 27$ C lines. The magnetic moments for each structure are shown as arrows on the corresponding atoms.

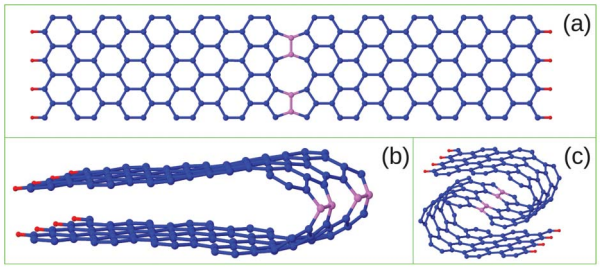

Fig. 2 A GNR with $N = 20$ C lines and pentagon/octagon defective line in the center for: (a) unfolded; (b) single folded; (c) double folded cases.

3 Results and discussion

In this work we consider zigzag GNRs with $10 \leqslant N \leqslant 27$, for which single folded structures are found to be stable. Double folds, however, exist for $N \geqslant 18$ and here we investigate structures with $18 \leqslant N \leqslant 27$. The studied systems were relaxed within the criteria specified above and some representatives are shown in Fig. 1 after relaxation. We consider the magnetic state of each structure by performing self-consistent relaxations with ferromagnetic (FM), antiferromagnetic (AFM), and nonmagnetic (NM) ordering. It turns out that for all unfolded and double folded ribbons, the ground state is always AFM. For single folds with odd N, the ground state is always AFM, while the ground state for even N is always NM. In all cases, the FM state is found to be least stable (the total energy is about 15 meV higher than the most stable configuration), thus it is not considered further. The folded structures are found to be stable due to the balance between the elastic bending from the curved regions and the vdW force from the flat-like portions. The elastic bending resists the curving, while the vdW attraction favors it. The shape of the single folds looks like a racket, but for $N < 21$ ($W < 43$ Å) the racket does not have a ''handle'', which is its flat-like portion. For larger ribbons, the flat portions are bigger and the curved regions are slightly reduced, which causes the configurations to be more stable.

We note that for the cases of armchair single folds,[12] there is an abrupt geometrical transition at $N = 28$ carbon lines ($W = 33$ Å), where the folded ribbon experiences a significant reduction of the curved region (by $\sim 1/2$) and increase in the ''handle'' (by ~ 2) as compared to $N = 27$. For the zigzag single folds, however, there is a gradual transition as the shape of the curved region remains practically constant, but the size of the parallel parts increase gradually.

Of particular interest is the variety of stacking patterns one achieves by such fractional nanotubes. For example, AA stacking is found for all even N 1 folds, while the pattern for all odd N is the one shown in Fig. 1b, which is called AB'.

Other variations can be found in the 2 folds. We point out that achieving different CC ring orientations in layered graphene systems maybe difficult to obtain experimentally, however, folding seems to provide many possible ways of obtaining layered registry dependence. For the asymmetric 1 folds, by changing the size of the overlap region we can also obtain various types of stacking patterns. The natural form of bilayer graphene and graphite is the Bernal (AB) stacking. However, other patterns have been seen in scanning tunneling microscopy imaging due to misaligned or twisted graphene layers.[20] Different patterns in such graphene layered systems can lead to modifications in their electronic and optical properties.[21,22]

We also simulate unfolded, single and double folded structures for a GNR with N = 20 zigzag lines and with an extended linear defect comprised by octagon/pentagons patterns positioned in the center. This line defect breaks the CC hexagonal symmetry and the curvature is reduced as compared to the defect free case. However, the double fold geometrical form is practically unchanged since the line defect is in the center of the ribbon Fig. 2.

The energetics for the studied zigzag GNRs is further investigated. In Fig. 3a, we show $\Delta E = E_{AFM} - E_{NM}$, which is the difference between the total energies for the AFM and NM ground states for the 0, 1, and 2 folded structures. The figure shows that the ground state for all unfolded and double folded GNRs is AFM. The C atoms at the very ends are found to have magnetic moments with magnitude $m = 0.16\mu_B$ (μ_B is the Bohr magneton). The magnetic moment strength quickly decreases towards the middle of the ribbon (Fig. 1). The value of m here is compatible with the value found by M. Fujita *et al.* ($m = 0.19\mu_B$) in.[3] For the 1 folded ribbons with even N, however, the ground state is always found to be nonmagnetic. We note that for such 1 folded ribbons, the AA stacking pattern causes the edge C atoms from the two sublattices residing on the two flat portions to be directly above each other, while for odd N the AB' stacking is realized (Fig. 1b). Consequently, the first type of registry dependence destroys the AFM ordering, while the second one does not. We further note that the symmetric ribbons with a line defect experience the same magnetic ordering as the corresponding defect-free ones do. Since N is even, the 1 folded defective ribbon is nonmagnetic, while the 0 and 2 folded ribbons maintain their edge AFM moments. This indicates that the defect line in the center does not influence the edge magnetism of the graphene nanostructures. The asymmetrically single folded structures preserve the localized edge moments for all N, since the edge atoms from the opposite sublattices/flat regions are never above each other.

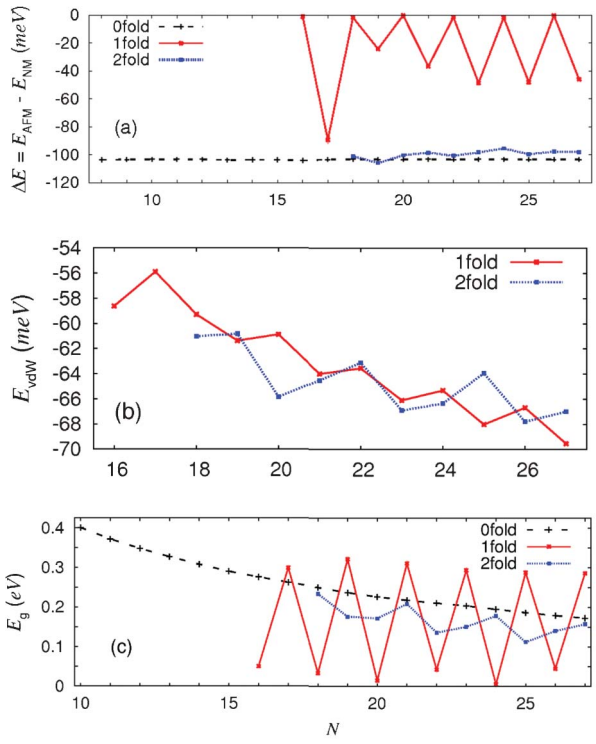

Fig. 3 (a) Difference in energy between an AFM (E_{AFM}) and nonmagnetic (E_{NM}) ground states for 0 fold, 1 fold, 2 fold zigzag GNRs as a function of N; (b) vdW energy E_{vdW} as a function of N for 1 fold and 2 fold GNRs; (c) Energy gap E_g as a function of N.

Fig. 3b shows how the vdW energy for each folded GNR changes as the width becomes larger. E_{vdW} increases as N grows, which is a consequence of the increase of overlap between the flat-like portions of each fold. The saw-tooth-like behavior of $|E_{vdW}|$ *vs.* N indicates a strong influence from the geometrical dependence of the interacting atoms.[23] Generally, we find that $|E_{vdW}|$ is smaller for even N as compared to the closest odd N cases for the single folds. For the double folds, the oscillatory-like pattern is characterized by a period of $N = 2$ separating the lowest and highest points of this functional behavior.

We also investigate the electronic structure for the different folds by examining their energy gaps. Fig. 3c shows that all studied unfolded ribbons are semiconductors with gradually decreasing energy gaps E_g as the width of the ribbons increases. All the double folds are also semiconductors, however, their energy gaps differ significantly for some N from the smooth E_g decrease for the unfolded ribbons. For single folds, only the ones with odd N are semiconductors. Interestingly, most of the nonmagnetic 1 folds of even N have been found to be semi-metals. We note that some of the armchaired 1 folds,[12] which are nonmagnetic, are also semimetal, but no such clear pattern as the one for the zigzag 1 folds was established. Fig. 3c reveals an oscillatory-like behavior following the pattern for the vdW energy. For example, 1 fold GNRs have larger gaps for odd N (corresponding to smaller $|E_{vdW}|$) as compared to the cases of even N (corresponding to larger $|E_{vdW}|$).

The characteristic energy band structure for some structures is given in Fig. 4. The energy gaps appear at the k-point of the GNR Brillouin zone. The two parallel-like energy levels which are closest to the Fermi level are determined by the edge π states. Upon folding, the interaction between the flat portions causes these energy bands to move closer in some cases or farther apart in others from the Fermi level, while the

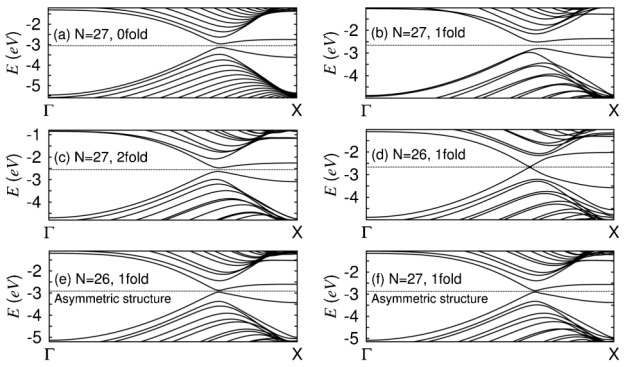

Fig. 4 Energy band structures of the unfolded, single and double folded GNRs with $N = 27$ carbon lines, the single folded GNR with $N = 26$, and the asymmetric single folded GNRs with $N = 26$ ($N_t = 3$; $N_b = 10$) and $N = 27$ ($N_t = 4$; $N_b = 10$), as indicated in each panel.

bending from the curved regions has only a secondary effect. Taking into account the vdW interaction can influence the overall interlayer coupling. This can have quite a profound effect on the energy gaps and the characteristic behaviour of the low lying energy states for 0 fold, 1 fold, and 2 fold. The band structure for the asymmetrically folded ribbons is not changed significantly upon varying the N_t and N_b for the considered cases. The vdW correction is taken into account self-consistently, therefore the relaxation of the structures will be affected at each step and it may contribute to changes in the bond-lengths, curvature of the folded parts and equilibrium distances. Comparing these results to the energy band structure for the folded armchaired GNRs,[12] one finds that no metal-semiconductor transition are found for the zigzag folds. For the armchair folds, however, a rich picture of several such transition was uncovered. This includes closing the energy gaps at different locations, and lifting the degeneracy of several bands.

Finally, we investigate the electronic structure of the unfolded, single and double folded GNRs for the particular case of a ribbon with $N = 20$ zigzag lines and with an octagon/pentagon topological defect line in the middle. The energy band structures and corresponding densities of states are calculated and shown in Fig. 5. We find that the magnetic ordering is not influenced by the line defect, as the magnetic edge states maintain the pattern found for non-defective structures. However, other researchers have shown that various locations of the line defect with respect to the edges and/or the presence of strain can lead to half-metallic or ferromagnetic behavior.[24,25]

The defect line destroys the particle-hole symmetry for the perfect $N = 20$ ribbon and lifts the degeneracy of the bands around the Fermi level, as seen in Fig. 5(a). The lowest valence and highest conduction dispersionless bands are due to the localized states at the octagon/heptagon line, while the next closest to E_F bands are due to the states localized at the edges. Very similar characteristics are found for the double folded ribbon (Fig. 5(c)) with the small difference that the flat bands

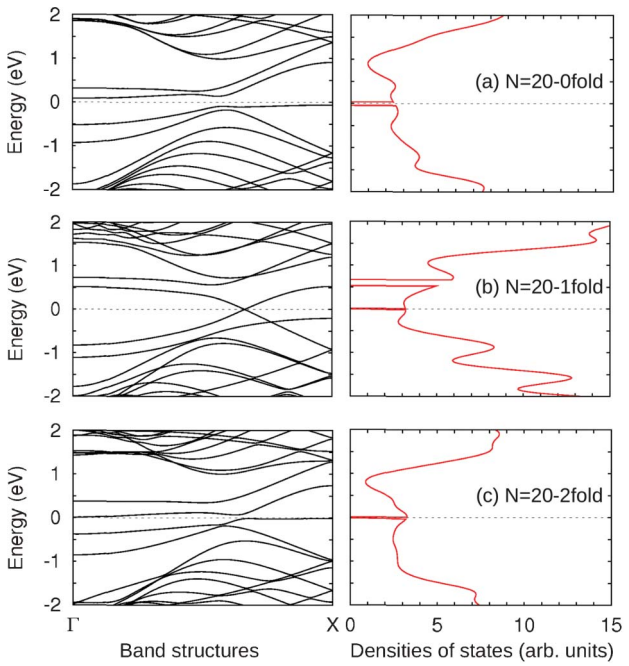

Fig. 5 Band structures and densities of states of the unfolded, single and double folded ribbons (as indicated in the right panel of each row) with $N = 20$ and with a line defect in the middle.

now reside on the Fermi level. The interaction between the flat portions in the single folded structure, however, affects the band structure in a profound way. The dispersionless bands are pushed above the E_F. The energy levels around the Fermi level are still composed of the localized states at the defect line, but they cross at $k = 0.33 \times \frac{\pi}{a}$, where a is the length of the lattice vector. In fact, the band structure for the single folded defective ribbon is very similar to the one found in single walled armchaired carbon nanotubes (see,[26] for example). Although, the energy bands in both cases have similar behavior, the crossing at $k = 0.33 \times \frac{\pi}{a}$ for the armchaired nanotubes is due to the zone folding due to the cylindrical boundary conditions. For the single folded ribbons, this is due to the topological defect line in the center of the ribbon together with the interaction between the parallel-like regions.

4 Conclusion

In this work, we present DFT calculations investigating zigzag-edged GNRs with single and double closed edges. The DFT approach is augmented self-consistently *via* a semiempirical correction (DFT-D2 dispersion correction) in order to take into account the van der Waals interactions. Some asymmetric and topological line defective structures are also considered. We obtain the equilibrium configurations for various folds and compare with similar ones for armchaired ribbons. We find that the zigzag folded ribbons have a variety of stacking patterns, which strongly affect the dispersive van der Waals contribution to the total energy. These registry dependent

effects are also important for the energy band gap and electronic structure modifications as a result of the folding process. The energy band structure and the magnetic states of the various structures are also analyzed. Modifications in the electronic structure originating from extended defect octagon/heptagon lines and folding are also found. Our studies present a comprehensive description of the interplay between mechanical alterations and electronic structure modifications in graphene nanoribbon structure. Our results can be of interest to researchers searching for ways to engineer graphene/graphene nanoribbon properties taking advantage of the out of plane flexibility of these nanostructured systems.

Acknowledgements

We acknowledge financial support from the US Department of Energy under Contract DE-FG02-06ER46297. We also acknowledge the use of the services provided by the University of South Florida Research Computing facilities.

References

1 K. S. Novoselov, D. Jiang, F. Schedin, T. J. Booth, V. V. Khotkevich, S. V. Morozov and A. K. Geim, *Proc. Natl. Acad. Sci. U. S. A.*, 2005, **102**, 10451–10453.
2 A. H. C. Neto, F. Guinea, N. M. R. Peres, K. S. Novoselov and A. K. Geim, *Rev. Mod. Phys.*, 2009, **81**, 109–162.
3 M. Fujita, K. Wakabayashi, K. Nakada and K. Kusakabe, *J. Phys. Soc. Jpn.*, 1996, **65**, 1920–1923.
4 L. Pisani, J. A. Chan, B. Montanari and N. M. Harrison, *Phys. Rev. B: Condens. Matter Mater. Phys.*, 2007, **75**, 064418.
5 Y.-W. Son, M. L. Cohen and S. G. Louie, *Phys. Rev. Lett.*, 2006, **97**, 216803.
6 L. Liao, Y.-C. Lin, M. Bao, R. Cheng, J. Bai, Y. Liu, Y. Qu, K. L. Wang, Y. Huang and X. Duan, *Nature*, 2010, **467**, 305–308.
7 J. Lahiri, Y. Lin, P. Bozkurt, I. I. Oleynik and M. Batzill, *Nat. Nanotechnol.*, 2010, **5**, 326–329.
8 Z. Liu, K. Suenaga, P. J. F. Harris and S. Iijima, *Phys. Rev. Lett.*, 2009, **102**, 015501.
9 J. Zhang, J. Xiao, X. Meng, C. Monroe1, Y. Huang and J.-M. Zuo, *Phys. Rev. Lett.*, 2010, **104**, 166805.
10 W. J. Yu, S. H. Chae, D. Perello, S. Y. Lee, G. H. Han, M. Yun and Y. H. Lee, *ACS Nano*, 2010, **4**, 5480–5486.
11 H.-V. Roy, C. Kallinger and K. Sattler, *Surf. Sci.*, 1998, **407**, 1–6.
12 N. B. Le and L. M. Woods, *Phys. Rev. B: Condens. Matter Mater. Phys.*, 2012, **85**, 035403.
13 G. Kresse and J. Furthmuller, *Phys. Rev. B: Condens. Matter*, 1996, **54**, 11169.
14 P. E. Blochl, *Phys. Rev. B: Condens. Matter*, 1994, **50**, 17953–17979.
15 J. P. Perdew, K. Burke and M. Ernzerhof, *Phys. Rev. Lett.*, 1996, **77**, 3865–3868.
16 T. Bucko, J. Hafner, S. Lebegue and J. G. Angyan, *J. Phys. Chem. A*, 2010, **114**, 11814–11824.
17 X. Wu, M. C. Vargas, S. Nayak, V. Lotrich and G. Scoles, *J. Chem. Phys.*, 2001, **115**, 8748–8757.
18 S. Grimme, *J. Comput. Chem.*, 2004, **25**, 1463–1473.
19 S. Grimme, *J. Comput. Chem.*, 2006, **27**, 1787–1799.
20 A. Luican, G. Li, A. Reina, J. Kong, R. R. Nair, K. S. Novoselov, A. K. Geim and E. Y. Andrei, *Phys. Rev. Lett.*, 2011, **106**, 126802.
21 X. Zhonga, R. Pandeya and S. P. Karna, *Carbon*, 2012, **50**, 784–790.
22 C. J. Tabert and E. J. Nicol, *Phys. Rev. B: Condens. Matter Mater. Phys.*, 2012, **86**, 075439.
23 Y. V. Shtogun and L. M. Woods, *J. Phys. Chem. Lett.*, 2010, **1**, 1356–1362.
24 J. Bhattacharjee, *J. Chem. Phys.*, 2012, **137**, 094705.
25 X. Lin and J. Ni, *Phys. Rev. B: Condens. Matter Mater. Phys.*, 2011, **84**, 075461.
26 S. Reich, C. Thomsen and P. Ordejon, *Phys. Rev. B: Condens. Matter*, 2002, **65**, 155411.

